Exp Tech (2017) 41:365–375
DOI 10.1007/s40799-017-0180-7

Effect of Heat Treatment on Dynamic Tensile Strength and Damage Behavior of Medium-Fine-Grained Huashan Granite

Z.L. Wang[1] · G.Y. Shi[1]

Received: 15 August 2016 / Accepted: 24 March 2017 / Published online: 17 April 2017

Abstract In order to investigate the dynamic behavior of medium-fine-grained Huashan granite treated by different temperatures, the splitting tests on the granite specimens are carried out using an improved split Hopkinson pressure bar (SHPB). The dynamic force equilibrium condition in the specimen is basically satisfied. The results show that with increasing treatment temperature, the ultrasonic P-wave velocity decreases, while thermal damage accordingly increases. The damage evolution follows the logistic curve model. For a temperature at or below 500 °C, all the specimens break diametrically into two halves at relatively low impact velocities. As the impact velocity rises, the triangular crushed zones are observed at the two loading ends of the specimen. When the temperature exceeds 500 °C, the damage of the specimen becomes severe, and even completely pulverized under high impact velocity. There are good correlations between the splitting strength and the treatment temperature, the ultrasonic P-wave velocity as well as the thermal damage. In addition, the splitting strength is slightly abnormal at 100 °C, namely the strength becomes lower than that at room temperature with increasing impact velocity. Overall, the decay of the splitting strength with thermal damage for the treatment temperatures over 100 °C accords with the power function. Moreover, the splitting strength of specimen is sensitive to strain rate at high temperature, but the increasing rates are different under different ranges of temperature.

✉ Z.L. Wang
cvewzL@hfut.edu.cn

[1] School of Civil & Hydraulic Engineering, Hefei University of Technology, Hefei, Anhui 230009, People's Republic of China

Keywords Granite · Temperature · Impact velocity · Damage · Ultrasonic P-wave velocity · Splitting strength

Introduction

In general, rock falls into the category of brittle material. Its tensile strength is typically smaller than the compressive strength by an order of magnitude. When disturbed by dynamic loads from blasting, earthquake or rockbursts, the underground rock would be vulnerable to tensile failure [1, 2]. Tensile failure is also an important aspect in thermal fracturing of rock. In addition, drill-and-blast excavation generates dynamic waves in the rock mass that easily result in tensile fracturing. Therefore, research on various methods to measure dynamic tensile strength of rock materials, especially at/after high temperature, is important for their application in rock mass engineering and the development in rock mechanics [3].

The International Society for Rock Mechanics (ISRM) has suggested several methods for measuring tensile strength of rock [4]. Due to experimental difficulties in direct tensile test, indirect methods serve as convenient alternatives to measure the tensile strength of rock-like materials, such as the Brazilian disc test, the ring test and three-point bending test [5, 6]. These indirect methods are much easier and less expensive than the direct methods, and they have thus been widely used in laboratory experiments.

As is well known, multi-field coupling problem of rock under the effects of stress, temperature, and seepage has become a new research topic. Over the past few decades, great progress has been made in the characterization of rock tensile failure: Yu pointed out the deficiencies of the traditional Brazilian test, and proposed a corrected formula based on the tensile stress at the center of specimen ends [7]. Wang

et al. considered that the flattened Brazilian disc specimen had some advantages over the traditional complete disc specimen in the dynamic splitting test, and the size effect on the dynamic tensile strength was mainly caused by the fracture process zone ahead of the crack tip [2]. Cho et al. performed dynamic tension tests on granite and tuff to study the strain rate dependency of the dynamic tensile strength [8]. Vishal et al. investigated the static splitting strength of granite at the temperatures from 30 °C to 250 °C, and indicated that the splitting strength increased slightly for temperatures below 100 °C and began to decrease for higher temperatures [9]. Liu et al. reported that the dynamic splitting tensile strength of marble was greatly affected by temperature based on the split Hopkinson pressure bar (SHPB) tests on heat-treated specimens [10]. As for the dynamic tensile strength of rock, Huang et al. concluded that the saturated specimen had stronger rate sensitivity than the dry specimen, and the water softening factor decreased with the loading rate [11]. Wu et al. investigated the dynamic tensile failure of rock under static pre-tension, and found that rock dynamic tensile strength decreased with increasing the pre-tension, while the total tensile strength of the rock was roughly independent of the pre-tension [12]. Gomez et al. used the SHPB to explore the dynamic tensile property of granite with a pre-existing damage [13]. These previous works have indicated that the dynamic tensile strength of rock is influenced by many factors.

Due to its high compressive strength, low total porosity, good thermal conductivity and thermal stability, granite has been chosen as the host rock for many engineering applications like radioactive waste repository. However, to date, the dynamic tensile behavior of heat-treated Huashan granite has not been explored. In this study, the dynamic splitting tests on the granite specimens treated by different temperatures are carried out using the improved SHPB. The ultrasonic P-wave velocity, the evolution of thermal damage and the failure mode of the specimen are analyzed to characterize the dynamic features of the granite. Moreover, the effects of treatment temperature, thermal damage and strain rate on the splitting strength of the specimen are investigated.

Specimen Preparation and Experiment Setup

Specimen Preparation

The rock specimens were prepared using Huashan granite taken from the Huashan region of Shanxi province of China. In general, Huashan granite has a gray and lumpy structure, classified as medium-fine-grained biotite granite. The main mineral compositions include microcline (41%), plagioclase (27%), quartz (22%) and biotite (7%) and others. The uniaxial compression strength and average density of the granite are 138 MPa and 2620 kg/m^3, respectively.

Cylindrical cores with a diameter of 50 mm were drilled from a big rock block. Then, the cores were cut into circular discs with thickness of ~25 mm. The two end planes of each specimen were ground to ensure that both planes were parallel with accuracy of ±0.05 mm and both planes were perpendicular to the longitudinal axis with accuracy of ±0.25°. These dimensions of the discs used for the subsequent dynamic splitting tensile tests conform to the standard suggested by the International Society for Rock Mechanics (ISRM) [4, 14].

In the present study, specimens were designed and grouped into six sets, including one obtained at room temperature and the other five treated at 100, 300, 500, 700, and 900 °C, respectively. Each set was tested with three (average) impact velocities (i.e. 5.4 m/s, 7.7 m/s and 13.7 m/s). In order to reduce the discretization of test data, each combination of temperature and impact velocity was tested on at least three specimens. The quality and geometry for all the granite specimens were carefully measured before and after heating.

Thermal and Testing Equipment

Granite specimens were heated in an electrical furnace (Fig. 1) at a rate of 10 °C/min until the desired temperature was reached. The temperature was maintained for 4 hours. Then, the furnace was cooled down to room temperature in more than 10 hours. All the treated samples were stored in a desiccator until they were tested.

Ultrasonic measurements of each specimen were completed using the contact transmission technique (Fig. 2) before and after the thermal treatment. Signals from the wave generator were transmitted to the specimen at one end via a transducer, picked up by a second transducer attached to another end of the specimen. The signals were then digitized and saved on the computer for obtaining the ultrasonic P-wave

Fig. 1 High temperature electric furnace

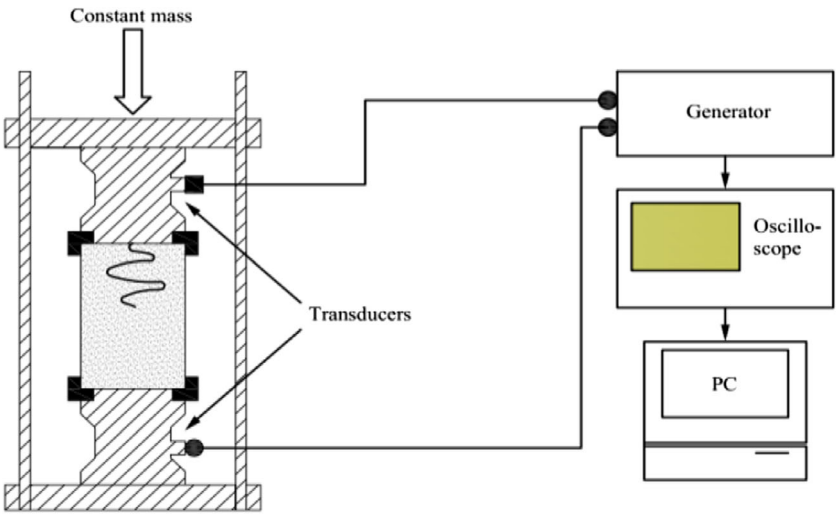

Fig. 2 Schematic of ultrasonic testing device

velocity (V_p). A constant pressure was systematically applied to ensure a tight contact between the sample and the transducers. Vaseline was chosen as coupling agent between specimen and transducers in order to transmit the ultrasonic energy to the specimen.

As shown in Fig. 3, the SHPB system is composed of elastic input (incident) and output (transmitted) bars with a short specimen sandwiched between them (Fig. 3(b)). The device incorporates a gas gun to accelerate the striker bar. The impact of the striker at the free end of the input bar develops a compressive longitudinal incident wave $\varepsilon_i(t)$. Once this wave reaches the interface between the input bar and the specimen, a part of it, $\varepsilon_r(t)$, is reflected, whereas another part $\varepsilon_t(t)$ goes through the specimen and transmits to the output bar. These three basic waves are recorded by the strain gauges mounted on the input and output bars. For the SHPB system used in this study, the lengths of the striker bar, incident bar, and transmitted bar are 400, 2400, and 1200 mm, respectively. The wave velocity of the bars is 5172 m/s and the elastic modulus is 210GPa.

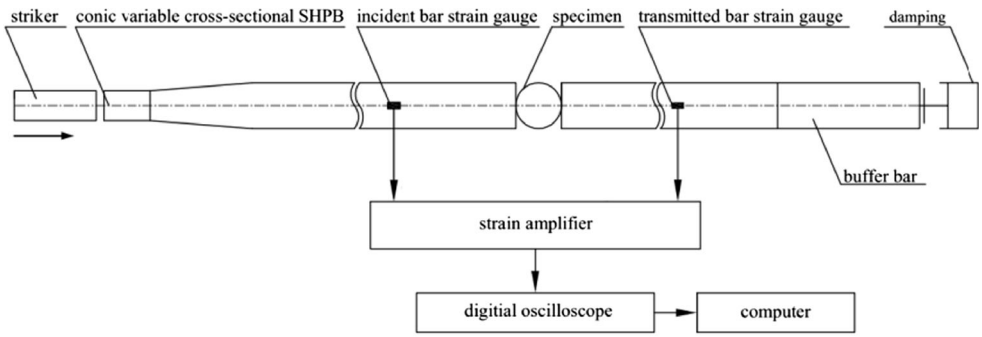

(a) Schematic of SHPB set-up

(b) Specimen state during testing

Fig. 3 The SHPB for dynamic indirect tensile test

The stress wave signals recorded in the SHPB tests are shown in Fig. 4. It can be seen that the magnitudes of incident wave for different treatment temperatures are very close under the same impact velocity, and the wave shape is similar to a bell-like waveform with a smoother and longer ramp. However, the transmitted waves and reflected waves are quite different. For example, at the treatment temperature of 700 °C the signal recorded on the transmitted bar is small, while the reflected wave signal accordingly becomes much stronger compared to that at 100 °C. This is due to the serious thermal damage of specimen at 700 °C, which makes it difficult for the stress-wave to propagate through the specimen.

Check of Dynamic Force Equilibrium

As mentioned above, granite is a brittle material with a low tensile strength, and usually it fails promptly at a small strain. Under high strain rate loading, if the loading waveform is not properly designed, the specimen may break at a moment when the incident wave is still rising and the force equilibrium has not been reached.

According to the wave propagation theory, the stress wave can be calculated from the corresponding strain signals measured by the strain gauges using the superposition principle. As thus, the stress in one section of the elastic incident bar is calculated from the two waves propagating in opposite directions in this section. Once the waves are known at bar-specimen interfaces, the forces at both faces of the specimen are given by the following equations:

$$F_1(t) = EA_0[\varepsilon_i(t) + \varepsilon_r(t)] \quad (1)$$

$$F_2(t) = EA_0\varepsilon_t(t) \quad (2)$$

where E and A_0 are, respectively, the Young's modulus and the cross-sectional areas of the bars.

To ensure that the uniform stress state, i.e., $F_1(t) = F_2(t)$, could be achieved as early as possible in specimens and that the amplitude of pulse oscillation could be reduced, soft rubber with the diameter of 10 mm and the thickness of 3 mm was employed as a pulse shaper through multiple trial tests [15]. In a traditional SHPB test, the incident wave with a sharp rising front may initiate undesired damage to the specimen upon impact. Consequently, the forces on both sides of the disc specimen are unequal, which is likely to result in misinterpretation of data. The pulse shaper allows the wave enough time to reverberate to-and-fro in the specimen, and this ideal bell-shaped waveform (see Fig. 4) makes it possible to produce a nearly uniform distribution of stress in the specimen after a very short time, which is about three times of the round-trip of stress wave in the sample [16].

Figure 5 shows the forces on the two loading sides of the specimens at the impact velocity of 7.7 m/s. For treatment temperatures ranging from 25 °C to 900 °C, the dynamic force on one side of the specimen F_1 is proportional to the sum of the incident and reflected waves, and the dynamic force on the other side F_2 is proportional to the transmitted wave. It can be seen that the dynamic forces on both sides of the specimens are almost identical before the specimen failure. The inertial effects are thus eliminated because there is no global force difference in the specimen. Consequently, the obtained results in this study are accurate and reliable.

Analysis of Physical Properties

Ultrasonic P-Wave Velocity of Specimen

Figure 6 plots the variation of ultrasonic P-wave velocity as a function of treatment temperature for the specimens. A reduction of the (average) wave velocity is noticed after heating due to the thermal damage. Before heat treatment, the velocities of P-wave are concentrated in a range of 3000 m/s ~ 3500 m/s. For specimens after heat treatment, it shows a slight decrease

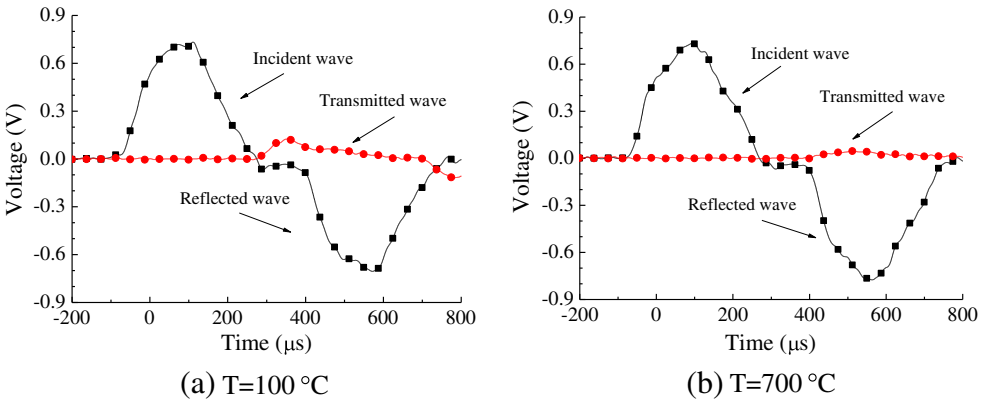

Fig. 4 Stress wave signals recorded in SHPB test

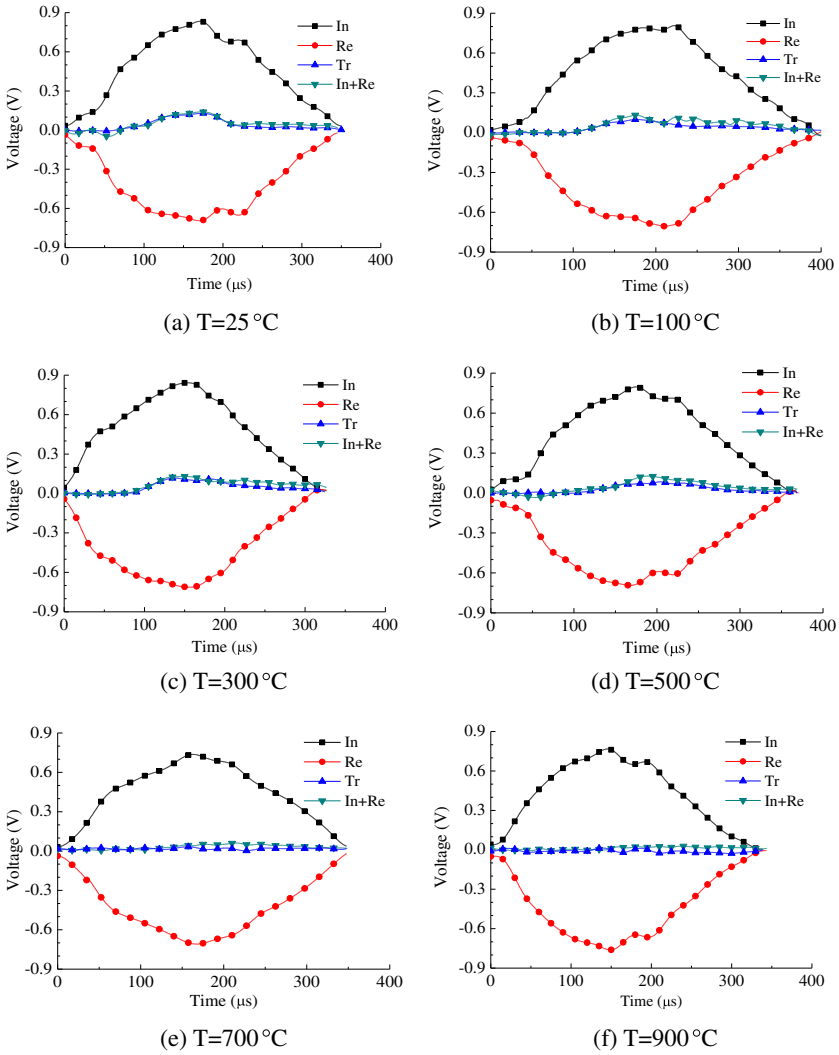

Fig. 5 Check of dynamic force equilibrium of specimen

of velocity between 25 and 100 °C. The difference between V_p before and after the treatment becomes obvious for temperatures ranging from 100 °Cto 700 °C. Once the temperature exceeds 700 °C, the ultrasonic P-wave velocity tends to remain stable, with an average value of 585 m/s at 900 °C. A comparison of the relationship between ultrasonic P-wave velocity and treatment temperature is given in Fig. 7. It is seen that the overall changing trend of the four different granite rocks is accordant, with a a sharp decrease at the temperatures of 500–700 °C [10, 17, 18].

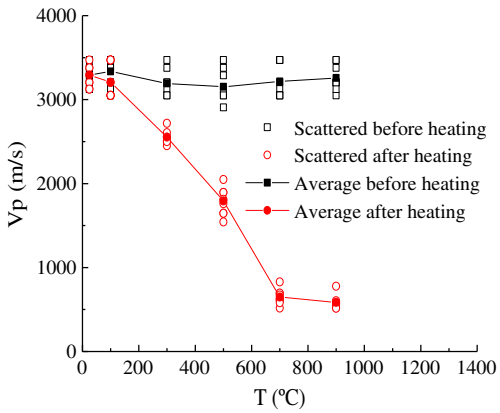

Fig. 6 Relation of ultrasonic P-wave velocity with treatment temperature

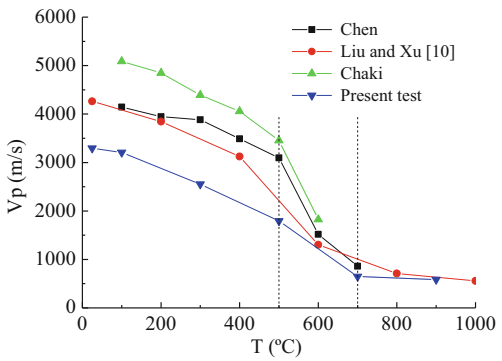

Fig. 7 Comparison of P-wave velocity of heated granite at different temperatures

The reason for the decrease of ultrasonic P-wave velocity is explained as follows: On one hand, the temperature action induces the evaporation of water, while it is well known that the wave velocity of water is five times that of air. Moreover, the microcracks resulting from gas expansion somewhat prevent the wave propagation and make the energy of wave attenuate rapidly. On the other hand, due to mineralogical heterogeneity of rock or phase transition of quartz at the temperature of 573 °C [19], the different coefficients of thermal expansion of quartz and other minerals lead to the coalescence of existing microcracks and initiation of new microcracks, which also causes the decrease of the ultrasonic P-wave velocity.

Analysis of Specimen Thermal Damage

The velocity of elastic wave is closely related to the rock damage. The relation between wave velocity and thermal damage can be expressed as:

$$D = 1 - \frac{\rho_1 c_1^2}{\rho_0 c_0^2} \tag{3}$$

where D is damage parameter; ρ_0 and ρ_1 are, respectively, the densities of granite specimen before and after heating; c_0 and $c_1$are, respectively, the elastic wave velocities of granite specimen before and after heating.

The logistic curve model was used in this study to correlate the thermal damage of specimens and the temperature of heat treatment. The model is originally used to delineate the population growth and is the basis of multi-species population dynamics, for example, the Lotka-Volterra models [20]. Herein, the logistical model was written as:

$$D = \frac{k}{1 + e^{\eta - \zeta T}} \tag{4}$$

where T represents heated temperature; η, ζ and k are constants.

Figure 8 shows the relation between the thermal damage D and the treatment temperature T. It can be observed that with the increase of treatment temperature, the thermal damage of specimen gradually increases. For the temperature ranging from 300 °C to 500 °C, there is a significant increase in thermal damage. As the treatment temperature increases to 700 °C, the thermal damage D approximates to a value of 1.0, and the sensitivity of thermal damage to treatment temperature greatly decreases. The parameters fitted from the test data are listed below: η=3.26877, ζ=0.00828 and k = 1.00036. The coefficient of correlation, R, is 0.989. It is seen that the logistic model can well reflect the non-linearity of thermal damage evolution of Huashan granite exposed to different treatment temperatures.

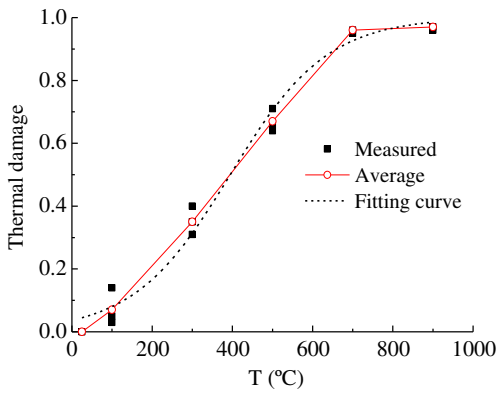

Fig. 8 Relation of thermal damage and treatment temperature

Characteristics of Failure Mode

The typical specimens that were recovered after the tests of six treatment temperatures ranging between 25 and 900 °C are shown in Figs. 9, 10, and 11 for impact velocities of 5.4 m/s, 7.7 m/s and 13.7 m/s, respectively. It can be seen that with the increase of the temperature and the same impact velocity, the degree of specimen failure becomes more severe. For a temperature ≤ 500 °C and an impact velocity of 5.4 m/s, all the specimens were split into two halves along the loading diameter after the tests (see Fig. 9). In addition to the main fracture, there were also some secondary fractures on the recovered specimens. These secondary fractures were induced by the load after the peak and will not affect the accuracy of the results [11]. With the increase of impact velocity, the microcracks did not have enough time to propagate and coalesce until failure, and thus the phenomenon of stress concentration took place. Before the formation of the main fracture, the compressive stress may have exceeded the compressive strength of granite, and the small triangle-shaped crushed zone was produced. It is also seen that the higher the impact velocity, the larger the triangular crushed zone. In particular, for the treatment temperatures above 500 °C, the granite specimens generally broke into several pieces of fragments. With the increase of the impact velocity of the striker bar upon the incident bar, the loading rate for the specimen gets higher, resulting in a higher stress concentration. This is why the angle of the crushed zone is larger at higher impact velocity.

Characteristics of Splitting Strength

As described above, the classical SHPB equations do not apply directly to this test due to the indirect load applied to the specimen. The force applied to the specimen was calculated using (equation (2)) with the transmitted bar measurements, and this can be converted to the tensile stress by the equation below:

$$\sigma_t = \frac{2F_2(t)}{\pi d L} = \frac{2EA_0\varepsilon_t(t)_{\max}}{\pi d L} \tag{5}$$

(a) T=25 °C (b) T=100 °C (c) T=300 °C

(d) T=500 °C (e) T=700 °C (f) T=900 °C

Fig. 9 Failure mode of specimen at impact velocity of 5.4 m/s

where L and d are, respectively, the thickness and diameter of specimen; $\varepsilon_t(t)_{\max}$ is the peak value of transmitted wave, as shown in Fig. 12.

To ensure the accuracy of the measurement results, some testing techniques (e.g. stress equilibrium for sample and slenderness ratio of sample) were adopted. The advantages of the method for measuring tensile strength are that the tensile failure is constrained to the center of the specimen and that the short Brazilian disc specimen can be used allowing the specimen to equilibrate over a transient period [21].

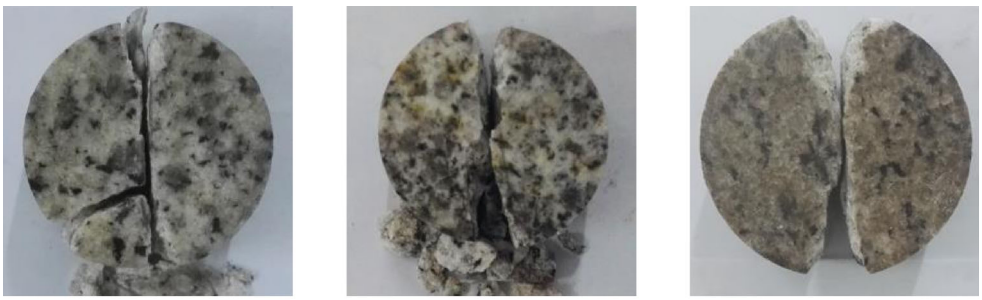

(a) T=25 °C (b) T=100 °C (c) T=300 °C

(d) T=500 °C (e) T=700 °C (f) T=900 °C

Fig. 10 Failure mode of specimen at impact velocity of 7.7 m/s

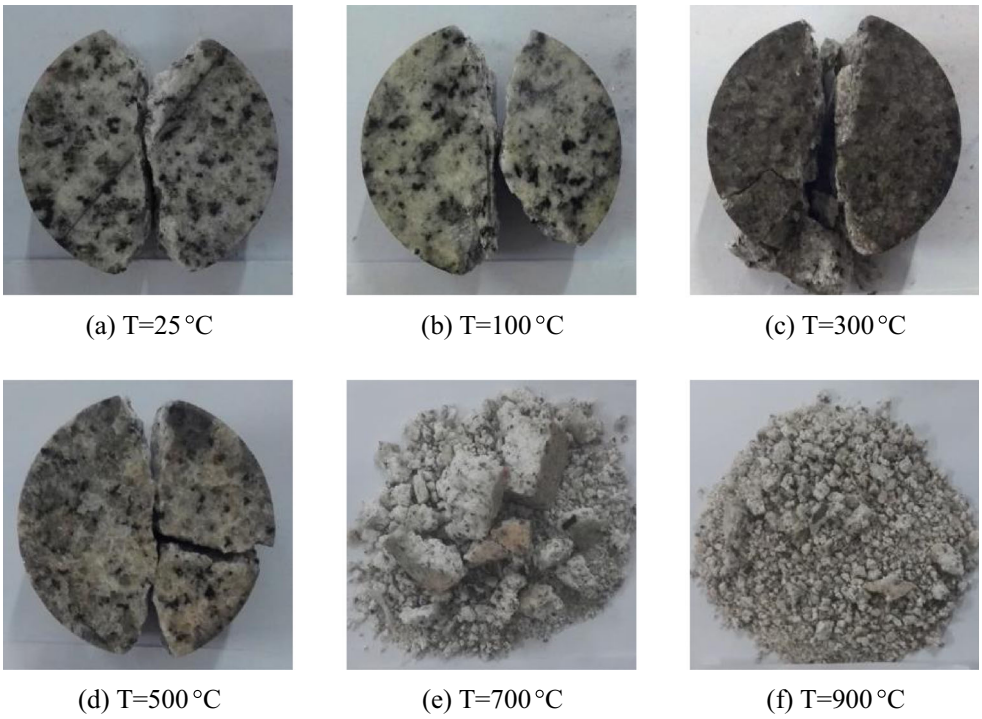

Fig. 11 Failure mode of specimen at impact velocity of 13.7 m/s

Effect of Treatment Temperature on Splitting Strength

Figure 13 presents the relation of splitting strength of granite to treatment temperature under different impact velocities. For each velocity, the splitting strength decreases with the increase of treatment temperature by a basically similar downward trend. The splitting strength of granite exhibits rate dependency, namely that the splitting strength increases with the strain rate (or impact velocity). At a low impact velocity of 5.4 m/s, the strength for the temperature of 100 °C increases slightly compared to that at room temperature (i.e. 25 °C). However, as the impact velocity increases, the contrary is observed. The larger the velocity is, the more obvious the phenomenon exhibits. This probably is due to the metamorphism and thermal expansion of internal mineral grains caused by heating. For a low impact velocity, the load does not exceed the load-bearing capacity of post-metamorphic mineral grains. In addition, the closure of microcracks and microvoids due to thermal expansion also leads to the slight increase of splitting strength. By contrast, at high impact velocities, once the impact action exceeds the load-bearing capacity of mineral grains, the rock is vulnerable to breakage, resulting in lower tensile strength at 100 °C than that at room temperature.

The comparison of the splitting strength of heat-treated Huashan granite with the granite rocks in other origins is shown in Fig. 13 [22, 23]. Generally, the curves of splitting tensile strength and treatment temperature show similar trends, and three phases can be identified: (1) treatment temperature between 25–100 °C, the splitting strength is volatile, which is significantly influenced by the impact velocity or

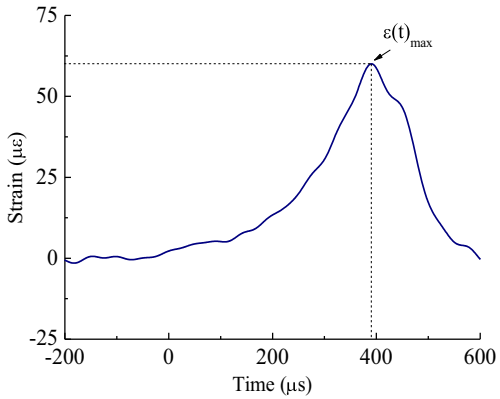

Fig. 12 Strain signal of typical transmitted wave

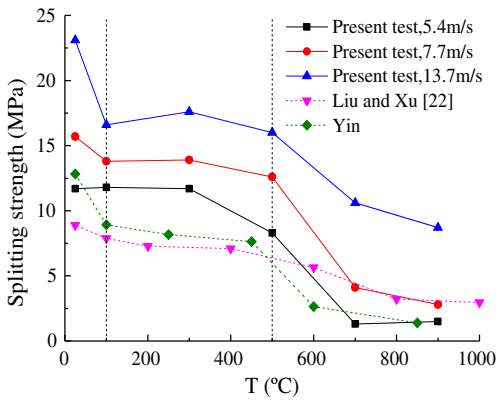

Fig. 13 Variation of splitting strength as a function of treatment temperature

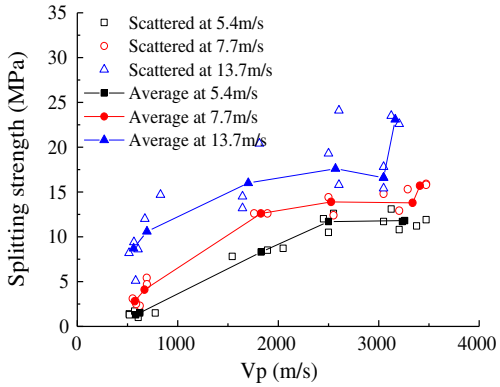

Fig. 14 Relation of splitting strength and ultrasonic P-wave velocity

loading rate; (2) between 100 °C to 500 °C treatment temperatures, the strength curve basically levels off or gradually changes; and (3) at treatment temperature of 500 °C or above, the splitting strength of granite decreases sharply.

Effect of P-Wave Velocity on Splitting Strength

In natural state, the velocity of ultrasonic P-wave is a comprehensive embodiment of the elastic coefficients, deformation characteristics and damage degree of rock material. The relationship between the rock strength and the P-wave velocity is statistically significant. The variations of splitting strength as a function of P-wave velocity for impact velocities of 5.4 m/s, 7.7 m/s and 13.7 m/s are shown in Fig. 14. It is clear that the splitting strength of granite decreases with decreasing ultrasonic P-wave velocity. Furthermore, the splitting strength is directly proportional to the impact velocity in a certain range.

Effect of Thermal Damage on Splitting Strength

The relationship between the splitting strength and thermal damage calculated from (equation (3)) is plotted in Fig. 15 for impact velocities of 5.4 m/s, 7.7 m/s and 13.7 m/s. It is seen that with the increase of thermal damage, the splitting strength of rock gradually decreases for the same impact velocity. Once the damage exceeds 0.6, the decrease of splitting strength is obvious. This is because the specimen is heavily fractured by thermal stress, leading to the coalescence and growth of microcracks and hence a considerable decline in the tensile strength. However, the strain rate effect still remains, as indicated by the increasing splitting strength of granite with the increase of the impact velocity of the striker.

In order to eliminate the influence of moisture content and better characterize the relation between splitting strength and thermal damage under different impact velocities, curves are fitted to the measured data above 100 °C, as shown in Fig. 15. It can be observed that with the increase of thermal damage, there is a rise in the decreasing rate of splitting strength. The relation between the splitting strength and thermal damage of the treated specimen can be expressed as a power law equation:

$$\sigma_t = a + bD^c \tag{6}$$

where σ_t is the splitting strength of granite; D denotes the thermal damage; a, b and c are fitting constants.

The constants from best fit are listed in Table 1. It turns out that the correlation coefficients, R, for three impact velocities are all quite close to 1.0, which implies the curve model represented by (equation (6)) can quite well correlate the relationship between the splitting strength of Huashan granite and the thermal damage for different impact velocities.

Relation of Splitting Strength with Strain Rate

Figure 16 presents the scatter diagram of splitting strength in terms of strain rate at different treatment temperatures. It indicates that the splitting strength increases linearly with the increase of strain rate for the same treatment temperature. The increasing rate of splitting strength of specimens exposed to treatment temperature at or below 500°C is significantly higher than those at the temperatures of

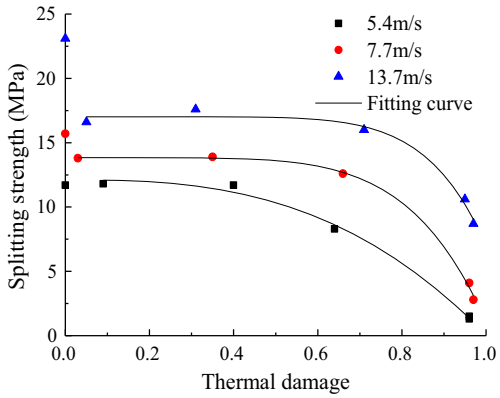

Fig. 15 Relation of splitting strength and thermal damage

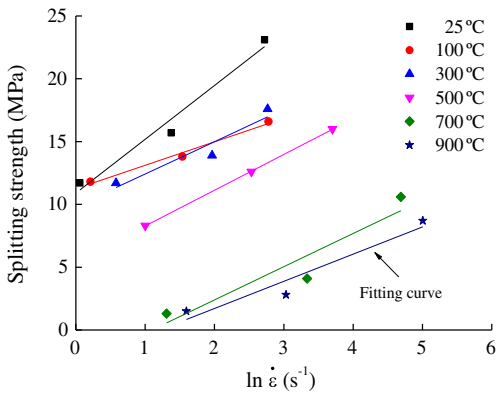

Fig. 16 Relation of splitting strength and strain rate

Table 1 Fitting constants for different impact velocities

Parameter / Velocity	*a*	*b*	*c*	*R*
5.4m/s	12.10217	-12.01404	2.77077	0.99086
7.7m/s	13.83445	-12.78514	5.80765	0.99595
13.7m/s	17.01764	-10.03994	7.50695	0.97291

700 and 900 °C. Additionally, the strain rate also increases with the increase of treatment temperature. As the treatment temperature increases from 500 °C to 700 °C, the increase of strain rate with temperature becomes very obvious, which implies that even at higher treatment temperature (≥700 °C), the splitting strength of granite still remains significant rate effect.

Conclusions

In this paper, a series of dynamic splitting tests on heat-treated Huashan granite have been performed to investigate its tensile strength and failure mode. According to experimental results, the major conclusions can be drawn as follows.

(1) At the treatment temperature of 500°C or below, the specimens are all fractured into two nearly equal halves divided along the loading diameter under low impact velocity, whereas the triangular crushed zones appear at the two loading ends of specimen with increasing impact velocity. When the temperature exceeds 500 °C, the damage of specimen becomes severe, and even pulverized under high impact velocity.

(2) The influence of treatment temperature on ultrasonic P-wave velocity is obvious. The value of Vp decreases with increasing temperature, and the influence becomes negligible when the temperature reaches 700 °C. The thermal damage of the granite can be fitted by a logistic curve model. For the treatment temperatures ranging from 500 °C to 700 °C, the damage shows significant increase, and it approaches to 1.0 at the temperature of 700 °C or above.

(3) At constant impact velocity, the splitting strength decreases with the increase of the treatment temperature. For the temperatures above 100 °C, the variation of splitting strength with thermal damage under different impact velocities follows the power law equation. The splitting strength of the tested granite shows rate dependency, and it increases linearly with the increase of strain rate to some extent.

Acknowledgements Financial support from the National Natural Science Foundation of China (51379147, 51579062) is greatly appreciated.

References

1. Li XB (2014) Rock dynamics fundamentals and applications. Science Press, Beijing, pp 208–209
2. Wang QZ, Li W, Xie HP (2009) Dynamic split tensile test of flattened Brazilian disc of rock with SHPB setup. Mech Mater 41:252–260
3. Wang ZL, Li YC, Wang JG (2008) A method for evaluating dynamic tensile damage of rock. Eng Fract Mech 75: 2812–2825
4. ISRM (1978) Suggested methods for determining tensile strength of rock materials. Int J Rock Mech Min Sci Geomech Abstr 15:99–103
5. Hudson JA, Rummel F, Brown ET (1972) The controlled failure of rock disks and rings loaded in diametral compression. Int J Rock Mech Min Sci Geomech Abstr 9:241–249
6. Coviello A, Lagioia R, Nova R (2005) On the measurement of the tensile strength of soft rocks. Rock Mech Rock Eng 38:251–273
7. Yu Y (2005) Question the validity of the Brazilian test for determining tensile strength of rock. Chin J Rock Mech Eng 24:1150–1157
8. Cho S, Ogata Y, Kaneko K (2003) Strain-rate dependency of the dynamic tensile strength of rock. Int J Rock Mech Min Sci 40:763–777
9. Vishal V, Pradhan SP, Singh TN (2011) Tensile strength of rock under elevated temperatures. Geotech Geol Eng 29: 1127–1133
10. Liu S, Xu JY (2015) An experimental study on the physic-mechanical properties of two post-high-temperature rocks. Eng Geol 185:63–70
11. Huang S, Xia K, Yan F, Feng X (2010) An experimental study of the rate dependence of tensile strength softening of Longyou sandstone. Rock Mech Rock Eng 43:677–683

12. Wu B, Chen R, Xia K (2015) Dynamic tensile failure of rocks under static pre-tension. Int J Rock Mech Min Sci 80:12–18
13. Gomez JT, Shukla A, Sharma A (2001) Static and dynamic behavior of concrete and granite in tension with damage. Theor Appl Fract Mech 36:37–49
14. Zhou YX, Xia K, Li XB, Li HB, Ma GW, Zhao J, Zhou ZL, Dai F (2012) Suggested methods for determining the dynamic strength parameters and mode-I fracture toughness of rock materials. Int J Rock Mech Min Sci 49:105–112
15. Frew DJ, Forrestal MJ, Chen W (2002) Pulse shaping techniques for testing brittle materials with a split Hopkinson pressure bar. Exp Mech 42:93–106
16. Frew DJ, Forrestal MJ, Chen W (2005) Pulse shaping techniques for testing elastic-plastic materials with a split Hopkinson pressure bar. Exp Mech 45:186–195
17. Chen SW, Yang C, Wang G (2016) Evolution of thermal damage and permeability of Beishan granite. Appl Therm Eng 110:1533–1542
18. Chaki S, Takarli M, Agbodjan WP (2008) Influence of thermal damage on physical properties of a granite rock: porosity, permeability and ultrasonic wave evolutions. Constr Build Mater 22: 1456–1461
19. Branlund JM, Hofmeister AM (2007) Thermal diffusivity of quartz to 1000°C: effects of impurities and the α-β phase transition. Phys Chem Miner 34:581–595
20. Li XY, Yin G (2016) Logistic models with regime switching: permanence and ergodicity. J Math Anal Appl 441:593–611
21. Xia KW, Yao W (2015) Dynamic rock tests using split Hopkinson (Kolsky) bar system-a review. J Rock Mech Geotech Eng 7:27–59
22. Liu S, Xu J (2014) Mechanical properties of qinling biotite granite after high temperature treatment. Int J Rock Mech Min Sci 71:188–193
23. Yin T, Li X, Cao W, Xia K (2015) Effects of thermal treatment on tensile strength of laurentian granite using brazilian test. Rock Mech Rock Eng 48:2213–2223